

Article

# Expressivity in Natural and Artificial Systems

Amy LaViers<sup>1</sup> \*<sup>1</sup> Mechanical Science and Engineering Department, University of Illinois at Urbana-Champaign

\* Correspondence: alaviers@illinois.edu; +1 (217) 300-1486

Version July 6, 2018 submitted to Nature

**Abstract:** Roboticians are trying to replicate animal behavior in artificial systems. Yet, quantitative bounds on capacity of a moving platform (natural or artificial) to express information in the environment are not known. This paper presents a measure for the capacity of motion complexity – the expressivity – of articulated platforms (both natural and artificial) and shows that this measure is stagnant and unexpectedly limited in extant robotic systems. This analysis indicates trends in increasing capacity in both internal and external complexity for natural systems while artificial, robotic systems have increased significantly in the capacity of computational (internal) states but remained more or less constant in mechanical (external) state capacity. This work presents a way to analyze trends in animal behavior and shows that robots are not capable of the same multi-faceted behavior in rich, dynamic environments as natural systems.

---

Abstractions about design goals such as form versus function help guide our thinking on constraining design spaces. In robotics, optimization is often used to define a notion of success motion; yet, robots suffer from brittle behaviors that break down in dynamic environments. In biology, natural selection is described via animal functionality inside a particular environmental context; yet, when individual animals are subjected to entirely new environments, they adapt [1]. Consider pavement ants (*Tetramorium caespitum*) brought to the low gravity environment of the International Space Station. This drastic change in environmental conditions produced climbing behaviors not observed by these individuals on earth, reminiscent of distant relatives (e.g., *Cephalotes goniodontus*), that proved effective in this new environment [2]. Would a purely functional, optimized pavement ant design be able to exhibit such climbing behavior? How can such capacity to adapt be described?

Animal movement encodes information that is meaningfully interpreted by natural counterparts [3]. This is a behavior that roboticians are trying to replicate in artificial systems. Can one artificial system successfully imitate another (possibly natural) system? Can a robotic system generate any arbitrary movement? The success of this goal is often determined through comparison of behavioral landmarks inside tight, well-crafted contexts [4] or through comparison to rough data capture of human counterparts [5] and other animals [6–8], with particular attention to the precision of end points of appendages [9–12] or rate of activity [13]. Imitating the movement of biological organisms, using similar metrics for success, has been a topic in animation [14] and robotics [15,16]. The review in [17] discusses “robots that imitate humans”, describing “very high fidelity playback.” In [18–23] motion capture data, a sparse representation, using a 10s or 100s of degrees of freedom, of human movement, seeds artificial system behavior. On the other hand, models in animation are orders of magnitude more complex, using 1,000s and 10,000s of parameters [24–26], occluding clear bounds on imitation of natural behavior. Prior work in robotics [27] and animation [28] have termed motion “expressive” or “affective”, which sets up a distinction between “function” and “expression” and is in contrast to work that shows the importance of context in resolving meaning in movement [29,30].

The duality between function and expression in motion (analogous to function and form in product design) is discussed in the Laban/Bartenieff Movement System [31,32]. Consider the same human motion in two distinct environments: a living room and a jungle. The agent *thrashes its*

*arms wildly, slashing at the air, and stomping its feet with heavy, sure-footed steps.* In the living room, this behavior may express anger to a human viewer, but in the jungle, this motion is needed to accomplish the function of progressing through the heavy undergrowth of the jungle, which would be apparent to a human viewer. This example establishes the idea that motion does not carry an inherent label, expression, or meaning even in the context of motion viewed by human counterparts. Instead, this paper will pose that a greater variety of movement profiles increases the functionality and expressiveness of a platform.

This brings to bear a notion of expressivity in movement that is consistent with usage in computer science [33], genetics [34], psychology [35], and dance [36]. Information theory gives a clear model explaining how an 8-bit display, made of three LEDs, is more *expressive* than a 1-bit display, made of one LED. Previous work in robotics [37,38] has explored how much information is needed in tasks of *sensing* the environment. Yet, quantitative bounds on capacity for *actuation* of a moving platform (natural or artificial) to express information in the environment are not known; it is an open question as to whether it is possible for artificial systems to recreate the motion of natural systems [39].

The paper points out the fundamental limitations on mechanization leveraging known limits on computation, previously proved by Turing [40], challenging the idea that natural and artificial motion are comparable, and uses a proposed static information-theoretic expressivity measure to create observations analogous to Moore's Law [41], contextualizing the practical mechanical capacity of robots. This analysis, applied to a variety of natural and artificial systems, shows trends [42,43] in increasing capacity in both internal and external complexity for natural systems while artificial, robotic systems have increased significantly in the capacity of computational (internal) states but remained more or less constant in mechanical (external) state capacity. This work shows that extant robots are not capable of the same multi-faceted behavior in rich, dynamic environments as complex natural systems and begins to quantify questions about the role of contextualized, redundant expression (as opposed to isolated, efficient function) in movement.

## 1. Mechanization: An Ideal Process With Limits

In [40] Turing outlines an *a-machine*, a machine with a finitely complex mechanical head along an infinite tape where symbols can be stored. The abstract machine requires the current configuration of the head, a list of basic instructions that tell the machine what to do in that configuration, and the complete configuration (state) of the whole thing. The components of an *a-machine* are given by the following list, loosely following [44]:

- a finite set of  $n$  machine states  $Q = \{q_1, \dots, q_n\}$ ;
- a finite set of  $m$  symbols  $\Sigma = \{\sigma_1, \dots, \sigma_m\}$ , e.g.  $\Sigma = \{0, 1, \epsilon\}$ , where the result of machine computation, a computable number, is recorded in binary with a blank option,  $\epsilon$
- an infinite "tape" where these symbols are recorded, comprised of cells  $c_1, c_2, c_3, \dots$ , which is often pre-populated with a finite sequence of symbols that will set up for desired behavior when the machine is in operation;
- current position along the tape, cell  $c_h$ , where  $h \geq 1$ ;
- a transition function  $\delta : Q \times \Sigma \mapsto Q \times \Sigma \times \{-1, 0, 1\}$ , which determines at a given state  $q_i$  for a given scanned symbol  $\sigma_i$  in  $c_h$  how to update the position of the head  $h$ , i.e., it moves left, stays in place, or moves right.

Future work would introduce various instantiations of this idea, including essential pieces of the modern computer such as stored program architecture and clocking. However, these add-ons do not change a central premise of Turing's paper: the capacity of computing machines. Specifically, he defines the class of numbers that can be computed by a properly formed (circle-free) machine to be enumerable (infinite but countable). That is, there are many, many more numbers that cannot be computed (e.g., irrational numbers without formulas for computation like  $\pi$ ) than can be. This is seen through application of Cantor's diagonal process, which shows that the correspondence between natural numbers and computable numbers is one-to-one (or that the set of real numbers and

computable numbers is not one-to-one) due to an inescapable recursive loop that traps an a-machine checking its own description number (this is known as the Halting Problem) [45]. That is, we can imagine many more numbers than machines can compute, which means we can imagine many more machine behaviors than machines can perform.

Now, to establish a way of thinking about machine movement (mechanization), invert the a-machine, establishing an æ-machine. In this abstraction the idea of a physical workspace replaces Turing's idea of "scratch paper" where computations could be worked out. An ideal mechanization machine will be able to complete tasks in the physical environment using extra workspace as needed. This is similar to (but certainly not the same as<sup>1</sup>) how a human artisan will use a workshop table during their work, placing part of a product off to the side while working on another element, using this tool or that to complete various steps, and increasing the size of their workshop as needed. Similarly, this machine can perform actions inside its workspace, layering simple actions in sequence to produce desired effect on the environment. Define such a machine as follows:

- a finite set of  $n'$  states  $Q' = \{q'_1, \dots, q'_n\}$ ;
- a finite set of  $m'$  actions, or *motion primitives*  $\Sigma' = \{\sigma'_1, \dots, \sigma'_m\}$ , e.g.  $\Sigma' = \{flexion, extension, e'\}$ , where the result of machine mechanization is executed as either moving, moving in the opposite direction, or doing nothing,  $e'$ ;
- an infinite "workspace" where these actions are executed, comprised of cells  $c'_1, c'_2, c'_3, \dots$ , which may be pre-populated with a finite set of primitives (or tools) that will set up for desired behavior when the machine is in operation;
- current position in the workspace, cell  $c'_{h'}$ , where  $h' \geq 1$ ;
- a transition function  $\delta' : Q' \times \Sigma' \mapsto Q' \times \Sigma' \times \{-1, 0, 1\}$ , which determines at a given state  $q'_i$  for a given motion primitive  $\sigma'_i$  in  $c'_{h'}$  how to update the position in the workspace  $h$ , which might be envisioned as a 1-, 2-, or 3-dimensional "tape".

What was a computation process (a sequence of logical symbols manipulated in an abstract, memory-like space) is now a mechanization process: a sequence of motion primitives executed in a discretized environment. This sequence is likewise represented as a number – one from Turing's set of computable numbers – showing the infinite, but enumerable, action sequences possible to be executed by æ-machines. Thus, æ-machines (idealized robots) have the same fundamentally limited capacity as a-machines (idealized computers). That is, *they cannot produce all the behaviors we might arbitrarily design*. In particular, the cardinality of behaviors is equal to the cardinality of the set of computable numbers and is many orders of magnitude smaller than the cardinality of the set of real numbers. Moreover, just as Turing established subroutines to build his Universal Machine, we can create more complex behaviors of motion primitives that fire in sequence together, acting as a *tool* in the workspace. In practice, that tool could be "software" (a stereotyped, preprogrammed gesture or action) or "hardware" (an end effector attachment as a CNC machine selects distinct cutting tools).

## 2. Static, Kinematic Capacity for A Mechanical Source

This discrete way of thinking immediately sets up a practical formalism for the concept of *expressivity*. In order to consider how complex the movement behaviors a machine can instantaneously exhibit are (independent of environment or further augmentation), note that a bounding *practical* limit on behavior is the cardinality of  $Q'$  or  $n'$ . While a robot with only a couple of degrees of freedom could split a given mechanization task into many steps, a robot with more might be able to do the entire task in one step<sup>2</sup>. (We see a similar parallel in computational devices.) Then,  $n'$  is a good bottleneck

<sup>1</sup> Indeed, unlike Turing, I want to motivate how this framework provides a *limiting* picture of machines rather than a mechanistic model for how humans (may) work, as analysis in [43] also motivates.

<sup>2</sup> Imagine a switchboard of buttons, which may be arranged in a manner advantageous to a particular platform morphology. In order to press one, two, three, four, and so on, buttons at the same time, a platform must have enough degrees of freedom (or the appropriate tool) to accomplish the task.

measure on *how complex* the instantaneous behavior of the machine can be (ignoring kinematically infeasible configurations and dynamic changes like velocity). Thus, let  $N$  be the number of actuator *types* on a machine. Let  $M_i$  be the number of degrees of freedom with a particular number of available configurations  $R_i$ , which is computed via counting from an actuators minimum to maximum range via its resolution where  $i = 1, \dots, N$ . From this description of a machine's construction, let

$$\mathcal{C} = \prod_{i=1}^N R_i^{M_i} \quad (1)$$

be the number of discrete geometric or kinematic configurations (shapes) available to a platform. From there the *kinematic expressivity* of that platform is the amount of information, or bits, needed to uniquely identify a configuration for that platform. This is given by

$$\mathcal{K} = \log_2(\mathcal{C}). \quad (2)$$

On a robot with a simple gripper (which is either open or closed), two identical servos, and a single LED  $N = 3$ . Assume each servo has  $360^\circ$  range and  $0.1^\circ$  resolution with a gripper that may be 'open' or 'closed' and an LED that may be 'on' or 'off',  $R_1 = 3600$  with  $M_1 = 2$  and  $R_2 = 2$  with  $M_2 = 2$ . This becomes

$$2^2 \times 3600^2 = 5.2 \times 10^7 \text{ configurations.}$$

This means the robot, as an information source, can express

$$\log_2(5.2 \times 10^7 \text{ configurations.}) \approx 26 \text{ bits}$$

of information, through state change, in its environment. Moreover, for this robot, most of its complexity comes from *mechanical* actuators. Removing the LED from the analysis gives a *kinematic mechanization capacity* of

$$\log_2(2^1 \times 3600^2 = 2.6 \times 10^7 \text{ configurations}) \approx 25 \text{ bits.}$$

Thus, this simplistic robot can be compared to a 25-bit display in terms of *mechanical* complexity.

Any computer that is Turing-complete can, in theory, compute the set of computable numbers, given enough memory and time. Similarly, a complete robot, with unlimited workspace and time, can produce a mechanization behavior associated with a computable number (i.e., it can simulate any  $\lambda$ -machine). However, the number of transistors in the CPU is a useful, implementation-specific measure (which has been growing [41]) of precision to understand how practically powerful a given machine is. Similarly, robots need more mechanical options in order to complete more complex mechanizations inside practical time and space limits.<sup>3</sup>

### 3. Computational and Mechanical Trends in Robotics

This measure and way of thinking about the duality of computation and mechanization can categorize artificial systems. The plot in Figure 1 shows the number of transistors in the onboard CPU of a range of robots over the past 15 years. Although, as many platforms are now internet connected, it is a limiting picture of the computational power available to these platforms. Plots like this have been used to track the progress of computational power over time, which has roughly doubled every year, even serving as a driving goal for the industry (Moore's Law [41]). In such plots each additional component on an integrated circuit represents the ability to represent a larger – or more precise – number on a single chip. Each new transistor adds a new power of 2 in representation precision. Note, that the *the number of transistors* in modern, stand-alone processors is in the billions. To convert that to

<sup>3</sup> This discrete view of robotic motion need not supplant the common practice of using a continuous vector-space model of configuration space [46]. Indeed, both abstractions can be useful.

possible machine configurations, where the actuators are transistors, the number 2 (which is the number of configurations for each actuator) has to be raised to that large number, resulting in a number of configurations that is bounded by  $2^{10^{11}}$  or  $10^{30102999566}$ . This number is an important, practical measure of how expressive the computers onboard robots are.

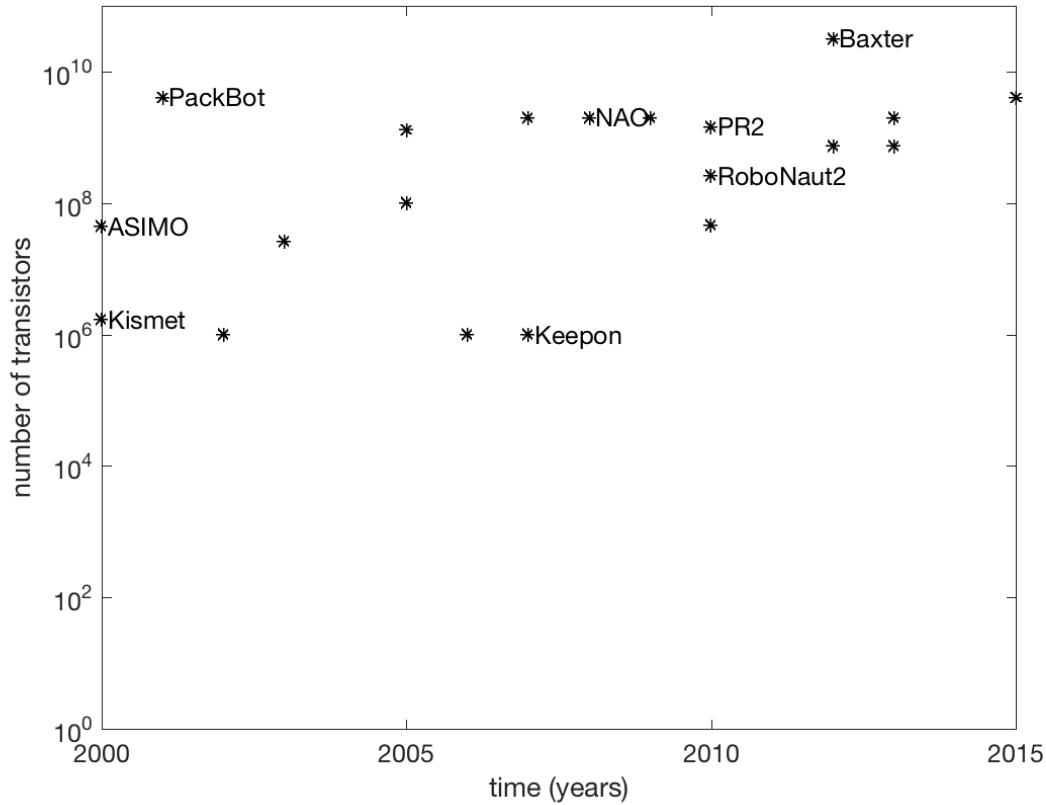


**Figure 1.** The number of transistors,  $t$ , used in computational processors of robots over the last fifteen years. The number of internal configurations available is then  $2^t$ . Some platform names are omitted for clarity; see Appendix for full list.

Figure 2 shows how this expressivity measure has evolved on robots over time. Specifically, the plot shows the number of possible kinematic configurations  $\mathcal{C}$  for a number of rigid-body robots whose motion is governed by motors and encoders over time. Like Moore's proxy of the number of transistors within a single chip, this kinematic configuration space is a static snapshot and does not account for dynamics, but it gives a starting point for measurement and comparison. Here, the corresponding practical measure of how externally expressive these robots are is bounded by  $10^{140}$ .

By converting the number of configurations  $\mathcal{C}$  to a number represented in a base 2 number system,  $\mathcal{K}$ , the change in the computational capacities of these platforms can be compared to their mechanization capacities as in Fig. 3. This log-log plot provides a comparison in terms of the number of bits which it would take to describe the largest number that would fit in the onboard CPU versus the number of bits needed to uniquely represent each pose. The plot shows a dramatic imbalance between computation and mechanization capacities and a flat trend in the order of magnitude of mechanical capacity over the past 15 years. Through this lens, the NAO Aldebaran, a small humanoid robot is comparable to a 1960s computer chip with only 256 transistors (see Appendix for detailed calculation).

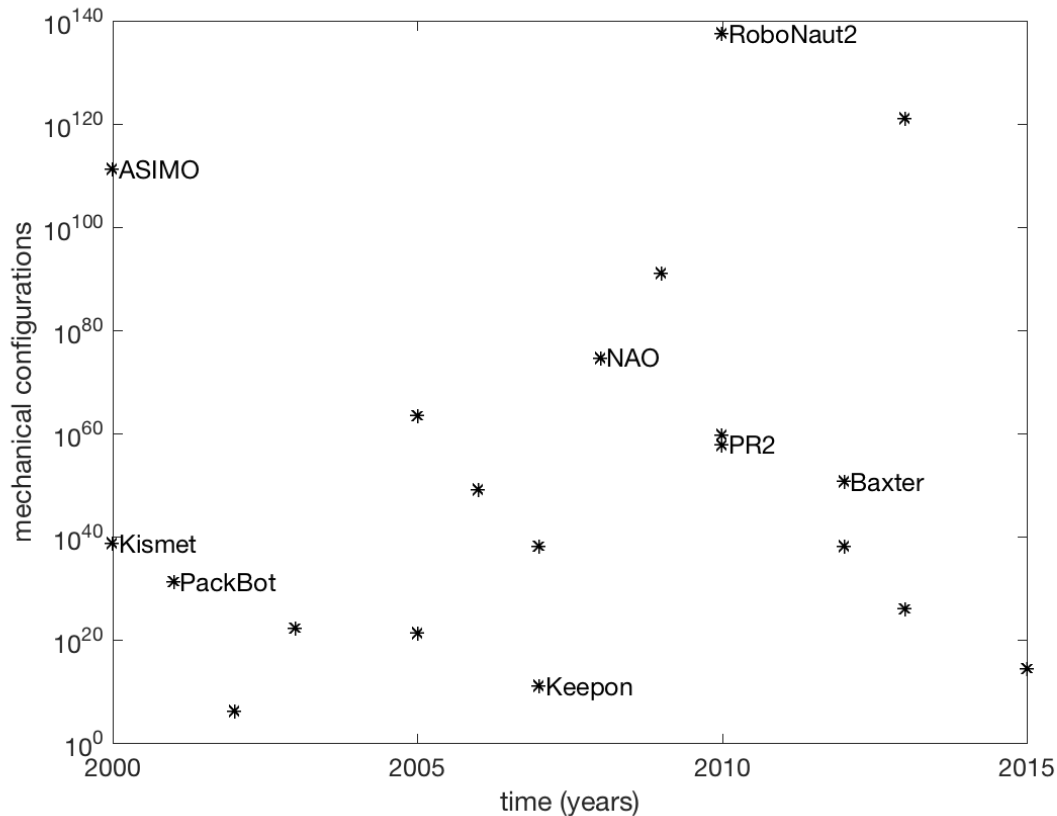


**Figure 2.** The number of external configurations available,  $C$ , for mechanization in robot platforms over time. Several platforms have been assumed to have a positioning resolution of  $0.1^\circ$  and an estimated range of motion. Some platform names are omitted for clarity; see Appendix for full list.

#### 4. A Comparison Between Machines and Animals

The previous section outlines a way to compare robot capacity for complex behavior, but the same method can be applied to biological creatures – with the caveat that such systems may involve processes not extant in today’s machines. Processes like “mechanization” and “computation” are not appropriate labels for natural systems, and the limit on behavior so carefully derived by Turing is not known to apply here. That is, the cardinality of the set of possible behavior of natural systems may (or may not) be larger than the cardinality of the set of computable numbers. However, we can loosely compare “computation” to internal state changes – those that do not meaningfully impact the environment – and “mechanization” to external state changes – those that cause change in the environment. Moreover, the difference between sensing and actuation blurs for these systems where movement is tightly linked to sensing, e.g. fovea and hairs.

In prior work, the movement of a *C. Elegan* was analyzed using a curve parameterized by 100 angles; then, after capturing an extended period of behavior on laboratory agar, a principle component analysis was performed, revealing that the structure of the behavior could be explained as a superposition of four primary poses [47]. Observing the animal through this lens provided new insights into the behavior of this well-studied animal [48,49], implying a meaningful parameterization, further explored in [50]. Stephen’s model can be used to compare the *C. Elegan* to modern robots. A *C. Elegan* has 302 neurons, which can be approximated to be either ‘firing’ or ‘not’ in a static snapshot of time. Then, each of the 100 angles have a typical range, shown in the empirical results in [47], between

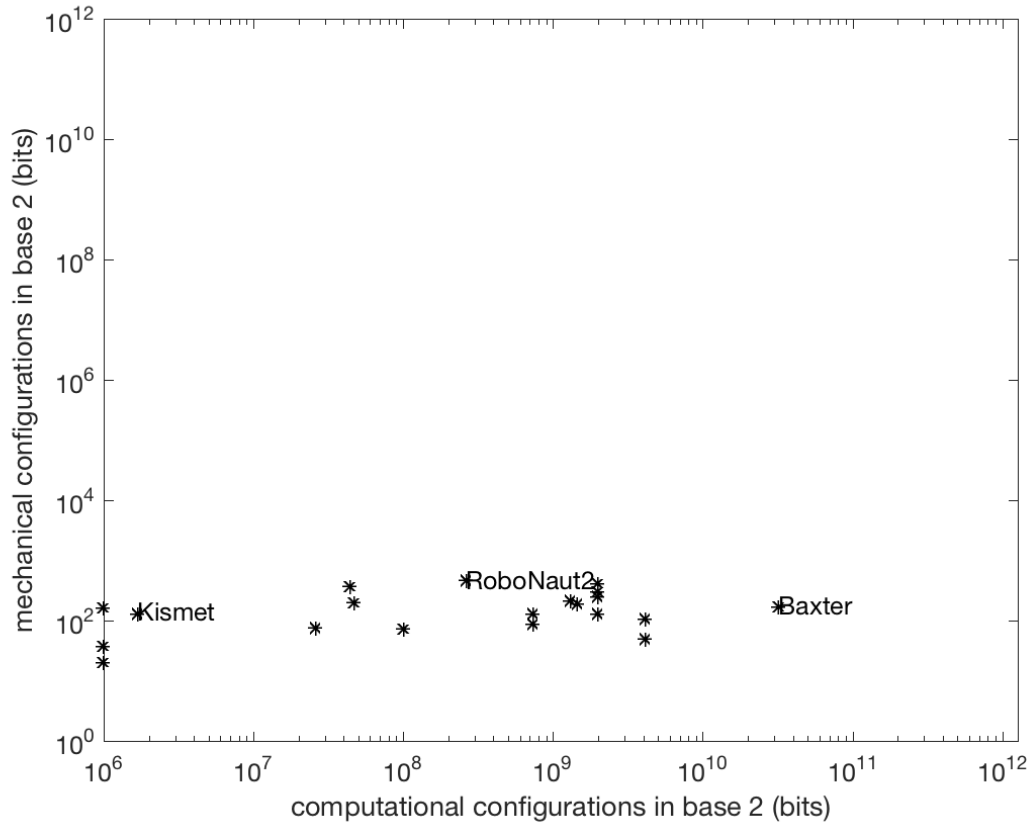


**Figure 3.** A comparison of computational complexity (# of transistors in the CPU) relative to mechanical complexity ( $\mathcal{K}$ ) on robotic platforms over time. Platform names are omitted for clarity; see Appendix for full list. The unit of measure on both axes is *bits*; a square plot highlights imbalance between internal and external states.

–1.5 radians to 1.5 radians, implying 0.1 radians of precision. Thus, using the metric proposed in Section 2, the kinematic mechanization capacity for this model of a simple animal can be calculated as

$$\mathcal{K} = \log_2(30^{100}) = \log_2(5.2 \times 10^{147} \text{ configurations}) \approx 491 \text{ bits.} \quad (3)$$

The linear model derived in [47] can also be used to derive a slightly more compact expression. Here, the idea is that it's possible that the organism, in a particular task or environment, does not utilize the full span of motion modeled by 100 angles. This could be a function of behavioral patterning, environment, or experimental set up<sup>4</sup>. Here, linear combinations four “eigenworms” describe 95% of the observed worm behavior. The weights on each eigenworm,  $\alpha_1$ ,  $\alpha_2$ ,  $\alpha_3$ , and  $\alpha_4$ , also have an observed range, which can be estimated from [47] as  $\alpha_1 : [-2, 2]$ ,  $\alpha_2 : [-2, 2]$ , and  $\alpha_3 : [-5, 5]$ . For the fourth, which was not found to have behavioral significance and is not provided in [47], assume  $\alpha_4 : [-2, 2]$ . For each, assume 0.1 in precision. This leads to the following calculation:

$$\mathcal{K} = \log_2(40^3 \times 100^1) = \log_2(6.4 \times 10^6 \text{ configurations}) \approx 23 \text{ bits.} \quad (4)$$

<sup>4</sup> However, like the pavement ant, the larger behavioral space intoned by the anatomical model may be used in future, unforeseen environments.

The summary of this analysis is plotted on Fig. 4. The plot gives a sense of the capacity of today's robots. It is shown that *C. Elegans* are apt natural analogs for the mechanical capacity of many robots. This does not mean that *C. Elegans* can do any of the specific functions that these robots can do; it means that they can do the same number things at the same time – or are as expressive. This is consistent with the fact that today's robots are created for single-tasks in limited environments. *C. Elegans* must forage for food and carry out other critical to life tasks in real, dynamic environments<sup>5</sup>.

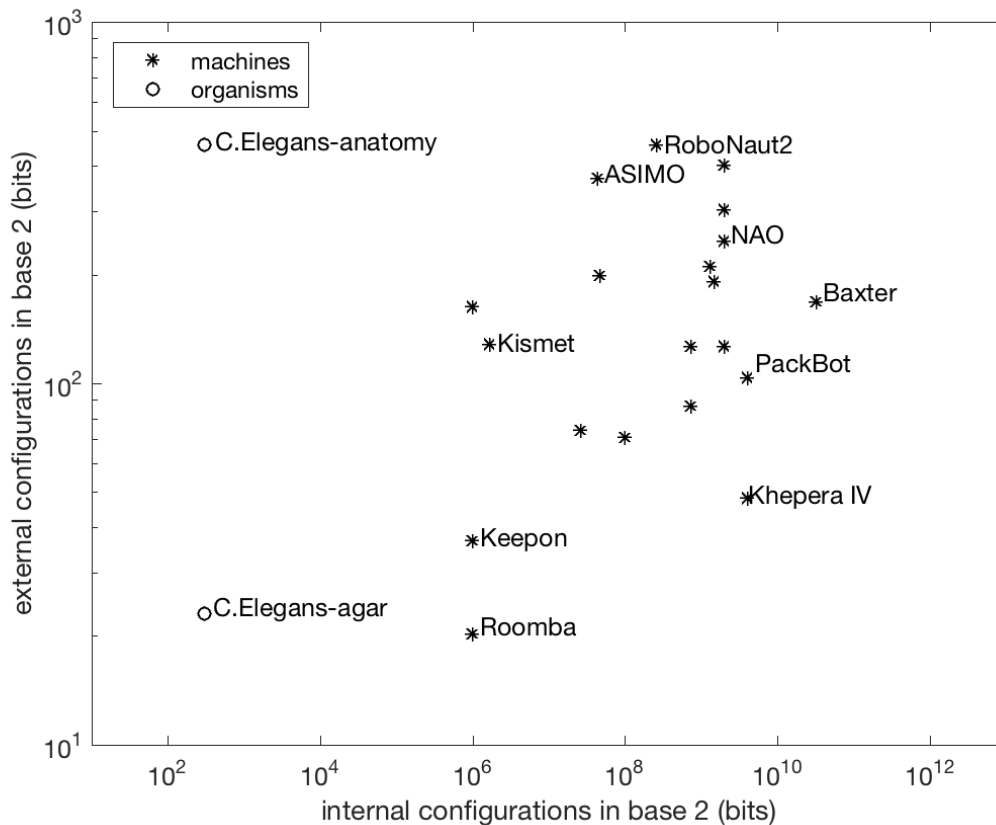


**Figure 4.** The machine data points are the same as those in Fig. 2. The *C. Elegans* x-axis points are based on the number of neurons (302). The y-axis data points plotted for *C. Elegans* show well-established behavioral models, one based on anatomy and the other based on exhibited behavior on agar [47].

Such detailed motion models for other animals are not common, but a few clear vignettes are appended to Fig 4 in Fig. 5. Relevant work done on fruit flies (*Drosophila*) abstracts their state as a vector with a heading over time [51], but an anatomical analysis via [52] can estimate instantaneous complexity of the organism. Researchers look to muscle activity involved in postural control for cats with weights having precision to the hundredth decimal place [53]; generalizing this precision to all estimated 517 [54] muscles in cats gives an estimate of the complexity of their muscular control, leaving out the mechanical advantages of their compliant bones, skin, and hair. For human motion, three different established guides to behavior (a public health diagnostic [55], a Natural Point OptiTrak motion capture file, and an animation of breathing [24]) of body posture can be used to show similarity between these models and those that identified behavioral understanding of *C. Elegans*. Either, humans are as externally complex as *C. Elegans* or more detailed models are needed.

<sup>5</sup> There are distinct Reynolds numbers at play. Inertial forces dominate the selected robots, while viscous forces dominate the motion of *C. Elegans*; however, this analysis is not considering forces, only the complexity of behavioral snapshots.



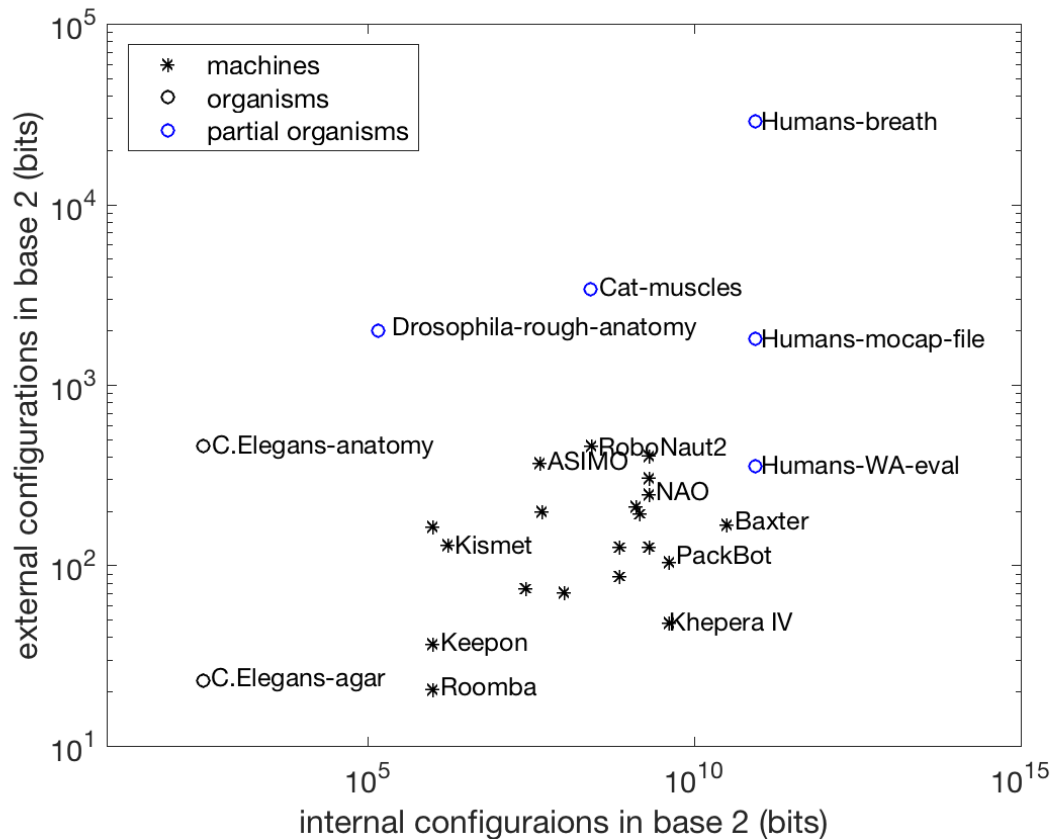


**Figure 5.** The data in Fig. 4 appended with data of a few more natural systems. The x-axis values for both of these organisms are based on the number of neurons [56]; the y-axis values are given by: Drosophila-rough-anatomy: analysis of [52]; Cat-muscles: generalizing the model of muscles in [53]; Humans-WA-eval: the structure of [55]; Humans-mocap: the structure of a Natural Point OptiTrack motion capture file; and Humans-breath: the simulation in [24]. See Appendix for more detail.

## 5. Conclusions

The paper has shown a relationship between mechanization and computation, pointing to a fundamental limit on machine behavior. The paper has introduced a static, practical measure for expressivity, clarifying prior points of view on function versus expression. Finally, the paper uses this work to compare extant artificial systems to natural systems, showing many modern robots, including humanoids, are about as expressive as a microscopic worm. This work is an essential piece of information in the discussion, which is by now mainstream, around the effect of machine-based automation of human tasks, particularly in manufacturing. Humans operate in dynamic environments where variability in movement is essential in accommodating and coping with an unpredictable world. Robots do well in repeatable tasks where environmental factors are controlled (as in a factory), but do not have the same capacity to adapt. The trends pointed to here in robotics may help guide system development: in hardware, soft and compliant robots, and, in software, increasing motion variability will offer robotic systems greater expressivity. Further, considering the wide, possibly unused, capacity for motion of natural systems, may produce improved understanding of how animals adapt both as individuals and as species.

## Acknowledgments

This work was funded by DARPA award #D16AP00001. Undergraduate students Jialu Li and Varun Jain helped collect and estimate data on each artificial platform reviewed.

## Appendix. Platform Details

Additional numbers used to calculate data points in Figures 1-3. For mechanical configurations, see below. Many of these were determined through observation and are meant to indicate the visual expressiveness of the platforms. Many rows represent multiple, homogeneous degrees of freedom (indicated through 'l/r' for 'left' and 'right' and with numbers in parenthesis) for space.

Robot & DOF	Range / Resolution	$R_i$
NAO		
l/r hand	open/close	2
head yaw	-119.5 to 119.5 / .1	2390
head pitch (at 0 yaw)	-38.5 to 29.5 / .1	680
l/r shoulder pitch	-119.5 to 119.5 / .1	2390
l/r shoulder yaw	-119.5 to 119.5 / .1	2390
l/r shoulder roll	-88.5 to -2 / .1	865
l/r wrist yaw	-104.5 to 104.5 / .1	2090
pelvis	-65.6 to 42 / .1	1076
l/r hip roll	-21.7 to 45.2 / .1	669
l/r hip pitch	-88 to 27.7 / .1	1157
l/r knee pitch	-5.3 to 121.0 / .1	1263
l/r ankle pitch	-68.2 to 52.9 / .1	1211
l/r ankle roll	-22.8 to 44.1 / .1	669
Baxter		
l/r S1	open/close	2
l/r E1	-2.864 to 150 / 0.1	1530
l/r W1	-90 to 120 / 0.1	2100
l/r S0	-97.5 to 97.5 / 0.1	1950
l/r E0	-175.0 to 175.0 / 0.1	3500
l/r W0	-175.25 to 175.25 / 0.1	3505
l/r W2	-175.25 to 175.25 / 0.1	3505
Khepera IV		
l/r wheel	360 / 0.1 / .1	3600
Roomba		
l/r wheel	360 / 0.1 / .1	3600
Kismet		
l/r ears pitch	-67.5 to 67.5 / 0.1	1350
l/r ears yaw	-22.5 to 22.5 / 0.1	450
l/r eyelids	-1.5 to 1.5 / 0.1	30
l/r brows pitch	-10 to 10 / 0.1	200
l/r lips	-30 to 30 / 0.1	600
jaw	-22.5 to 22.5 / 0.1	450
PR2		
l/r shoulder pan	170 / 0.1	1700
l/r shoulder tilt	115 / 0.1	1150
l/r upper arm roll	270 / 0.1	2700
l/r elbow flex	140 / 0.1	1400
l/r forearm roll	360 / 0.1	3600
l/r wrist pitch	130 / 0.1	1300
l/r wrist roll	360 / 0.1	3600
head pan	350 / 0.1	3500
head tilt	115 / 0.1	1150
Big Dog		
each leg (5) (x4)	150 / 0.08	1875

Robot & DOF	Range / Resolution	$R_i$
ASIMO		
head (3)	150 / 0.08	1875
arms (14)	150 / 0.08	1875
hands (4)	150 / 0.08	1875
torso (1)	150 / 0.08	1875
legs (12)	150 / 0.08	1875
Little Dog		
l/r front knee RY	-177 to 57 / 0.1	2340
l/r front hip RX	-34 to 34 / 0.1	680
l/r front hip RY	-200 to 137 / 0.1	337
l/r back knee RY	-57 to 177 / 0.1	2340
l/r back hip RX	-34 to 34 / 0.1	680
l/r back hip RY	-137 to 200 / 0.1	337
Robotnaut2		
head yaw/pitch/roll	150 / 0.08	1875
l/r hands (12)	150 / 0.08	1875
l/r arms (7)	150 / 0.08	1875
KeepOn		
tilt	-40 to 40 / 0.08	1000
pan	-180 to 180 / 0.08	4500
pon	0 to 100 / 0.08	1250
side	-25 to 25 / 0.08	625
RoboSapien		
l/r elbows	-90 to 90 / 0.1	1800
l/r shoulders	-30 to 150 / 0.1	1800
torso	-67.5 to 67.5 / 0.1	1350
l/r hips	-60 to 60 / 0.1	1200
Darwin		
neck pitch	-25 to 25 / 0.1	500
neck roll	-90 to 90 / 0.1	1800
l/r elbow	0 to 150 / 0.1	1500
l/r shoulder rotation	-100 to 100 / 0.1	2000
l/r shoulder compression	-15 to 15 / 0.1	300
l/r knee	0 to 150 / 0.1	1500
l/r foot	0 to 90 / 0.1	900
l/r waist rotation	-15 to 15 / 0.1	300
l/r knee/foot	-75 to 75 / 0.1	1500
l/r waist bend	0 to 100 / 0.1	1000
Aibo		
head pan	-89 to 89 / 0.1	1780
head tilt	-62.5 to 62.5 / 0.1	1250
head roll	-29 to 29 / 0.1	580
shoulders (4)	0 to 100 / 0.1	1000
torso	-117 to 117 / 0.1	2340
knees (4)	0 to 175 / 0.1	1750
l/r ears	0 to 20 / 0.1	200
tail (front to back)	-22.5 to 22.5 / 0.1	450
tail (left to right)	-12.5 to 12.5 / 0.1	250

<b>Robot &amp; DOF</b>	<b>Range / Resolution</b>	$R_i$
Packbot		
shoulder rot.	0 to 360 / 0.1	3600
shoulder pivot	0 to 220 / 0.1	2200
E1 pivot	0 to 340 / 0.1	3400
E2 pivot	0 to 340 / 0.1	3400
gripper rot.	0 to 360 / 0.1	3600
gripper I/O	180 / 0.1	1800
head rot.	0 to 360 / 0.1	3600
flipper	0 to 360 / 0.1	3600
Simon		
torso (2)	-75 to 75 / 0.1	1500
l/r arm (7)	0 to 200 / 0.1	2000
face (5)	0 to 200 / 0.1	2000
Cheetah		
hip rot. (4)	0 to 30 / 0.1	300
hip (4)	0 to 150 / 0.1	1500
knee (4)	0 to 200 / 0.1	2000
spine	-10 to 10 / 0.1	200
LBR iiwa		
axis 1	-170 to 170 / 0.1	3400
axis 2	-120 to 120 / 0.1	2400
axis 3	-170 to 170 / 0.1	3400
axis 4	-120 to 120 / 0.1	2400
axis 5	-170 to 170 / 0.1	3400
axis 6	-120 to 120 / 0.1	2400
axis 7	-175 to 175 / 0.1	3500
KR60HA		
axis 1	-185 to 185 / 0.1	3700
axis 2	-135 to 35 / 0.1	1700
axis 3	-120 to 158 / 0.1	1780
axis 4	-350 to 350 / 0.1	7000
axis 5	-119 to 119 / 0.1	2380
axis 6	-350 to 350 / 0.1	7000

For computational configurations, the following values were used. Here,  $C$  is  $2^x$  where  $x$  is the number of transistors. Indeed, often, another, larger computer (or cluster of processors) is networked to these machines through wireless or wired connections. But, it is instructive nonetheless to compare how much more sophisticated the computational power (even that which is on board) is relative to the mechanical power.

Robot	Processor	# of transistors
NAO	Atom Z530	4.7E+07
Baxter	3rd Gen Intel Core i7-3770	1.40E+09
Khepera IV	ARM Cortex-A8	2.00E+09
Roomba		1.00E+06
Kismet	Motorola 68332 (4)	1.68E+06
PR2	Two Quad-Core i7 Xeon (8 cores)	1.462E+09
Big Dog	Pentium CPU	1.30E+09
ASIMO	Pentium III-M 1.2 GHz	4.40E+07
Little Dog	Pentium CPU	2.00E+09
Robotnaut2		2.622E+08
KeepOn	PS234	1.00E+06
RoboSapien	200MHz ARM9	2.60E+07
Darwin	Intel Atom Z510	4.70E+07
Aibo	64 bit RISC	1.00E+06
Packbot	Pentium 3	4.50E+07
Simon		2.00E+09
Cheetah		7.31E+08
LBR iiwa		7.31E+08
KR60HA		1.00E+08

For the natural systems analyzed, the following values were used based on [24,47,52–55].

Organism & DOF ( $M_i$ )	Range / Resolution	$R_i$
<i>C. Elegan</i> (anatomy)		
$\theta$ (100)	-1.5 rad to 1.5 / 0.1	150
<i>C. Elegan</i> (agar behavior)		
$\alpha_1, \alpha_2,$ and $\alpha_4$	-2 to 2 / 0.1	40
$\alpha_3$	-5 to 5 / 0.1	100
<i>Drosophila</i>		
Tarsus 5 (6)	0 to 180° / 0.1°	1800
Tarsus 4 (6)	0 to 180° / 0.1°	1800
Tarsus 3 (6)	0 to 180° / 0.1°	1800
Tarsus 2 (6)	0 to 180° / 0.1°	1800
Tarsus 1 (6)	0 to 180° / 0.1°	1800
Tibia (6)	0 to 180° / 0.1°	1800
Femur (6)	0 to 180° / 0.1°	1800
Trochanter (6)	0 to 360° / 0.1°	3600
Coxa (6)	0 to 10° / 0.1°	100
Wing cells (12))	flexed or relaxed	2
Wing hinge (6)	0 to 180° / 0.1°	1800
Halteres (6)	0 to 360° / 0.1°	3600
Head, Thorax, Abdomen (9)	0 to 45° / 0.1°	450
Proboscis	in or out	2
Antennae (12)	0 to 10° / 0.1°	100
Bristles (200)	flexed or not	2
Hairs (1000)	flexed or not	2

Organism & DOF ( $M_i$ )	Range / Resolution	$R_i$
Cat		
Muscles (517)	0 to 1 / 0.01	100
Human (WA-eval)		
Each listed diagnostic [55] (37)	various / 0.1	various
Human (mocap)		
DOFs (66)	-180° to 180° / 0.000001	360000000
Human (breath)		
Muscle-spring elements (1500)	-1 to 1 / 0.000001	1000000

## References

1. Turner, J.S. Biology's second law. Homeostasis, purpose and desire. *Beyond mechanism. Putting life back into biology* **2013**, pp. 183–203.
2. Countryman, S.M.; Stumpe, M.C.; Crow, S.P.; Adler, F.R.; Greene, M.J.; Vonshak, M.; Gordon, D.M. Collective search by ants in microgravity. *Frontiers in Ecology and Evolution* **2015**, *3*, 25.
3. Laidre, M.E.; Johnstone, R.A. Animal signals. *Current Biology* **2013**, *23*, R829–R833.
4. Dragan, A.D.; Lee, K.C.; Srinivasa, S.S. Legibility and predictability of robot motion. Human-Robot Interaction (HRI), 2013 8th ACM/IEEE International Conference on. IEEE, 2013, pp. 301–308.
5. Ames, A.D. Human-inspired control of bipedal walking robots. *IEEE Transactions on Automatic Control* **2014**, *59*, 1115–1130.
6. Hopkins, J.K.; Spranklin, B.W.; Gupta, S.K. A survey of snake-inspired robot designs. *Bioinspiration & biomimetics* **2009**, *4*, 021001.
7. Haldane, D.W.; Peterson, K.C.; Bermudez, F.L.G.; Fearing, R.S. Animal-inspired design and aerodynamic stabilization of a hexapedal millirobot. Robotics and Automation (ICRA), 2013 IEEE International Conference on. IEEE, 2013, pp. 3279–3286.
8. Cully, A.; Clune, J.; Tarapore, D.; Mouret, J.B. Robots that can adapt like animals. *Nature* **2015**, *521*, 503.
9. UR5 Technical specifications. Technical report, Universal Robots, 2016.
10. JACO2 6 DOF Advanced Specification Guide. Technical report, Kinova Robotics, 2017.
11. Sawyer Collaborative Robot Tech Specs. Technical report, Rethink Robotics, 2018.
12. Meijer, J.; Lei, Q.; Wisse, M. Performance study of single-query motion planning for grasp execution using various manipulators. Advanced Robotics (ICAR), 2017 18th International Conference on. IEEE, 2017, pp. 450–457.
13. Hodson, R. How robots are grasping the art of gripping. *Nature* **2018**, *557*, S23–S25.
14. Reynolds, C.W. Steering behaviors for autonomous characters. Game developers conference, 1999, Vol. 1999, pp. 763–782.
15. Egerstedt, M.; Balch, T.; Dellaert, F.; Delmotte, F.; Khan, Z. What are the ants doing? vision-based tracking and reconstruction of control programs. Proceedings of the IEEE International Conference on Robotics and Automation (ICRA 2005), 2005, pp. 18–22.
16. Powell, M.J.; Zhao, H.; Ames, A.D. Motion primitives for human-inspired bipedal robotic locomotion: walking and stair climbing. Robotics and Automation (ICRA), 2012 IEEE International Conference on. IEEE, 2012, pp. 543–549.
17. Breazeal, C.; Scassellati, B. Robots that imitate humans. *Trends in cognitive sciences* **2002**, *6*, 481–487.
18. Yamane, K.; Kuffner, J.J.; Hodgins, J.K. Synthesizing animations of human manipulation tasks. ACM Transactions on Graphics (TOG). ACM, 2004, Vol. 23, pp. 532–539.
19. Nakaoka, S.; Nakazawa, A.; Yokoi, K.; Ikeuchi, K. Leg motion primitives for a dancing humanoid robot. Robotics and Automation, 2004. Proceedings. ICRA'04. 2004 IEEE International Conference on. IEEE, 2004, Vol. 1, pp. 610–615.
20. Gillies, M. Learning finite-state machine controllers from motion capture data. *Computational Intelligence and AI in Games, IEEE Transactions on* **2009**, *1*, 63–72.

21. Kulic, D.; Ott, C.; Lee, D.; Ishikawa, J.; Nakamura, Y. Incremental learning of full body motion primitives and their sequencing through human motion observation. *The International Journal of Robotics Research* **2012**, *31*, 330–345.
22. LaViers, A.; Egerstedt, M. Style-based Abstractions for Human Motion Classification. *ACM/IEEE 5th International Conference on Cyber-Physical Systems* **2014**.
23. Joo, H.; Liu, H.; Tan, L.; Gui, L.; Nabbe, B.; Matthews, I.; Kanade, T.; Nobuhara, S.; Sheikh, Y. Panoptic studio: A massively multiview system for social motion capture. Proceedings of the IEEE International Conference on Computer Vision, 2015, pp. 3334–3342.
24. Zordan, V.B.; Celly, B.; Chiu, B.; DiLorenzo, P.C. Breathe easy: model and control of simulated respiration for animation. Proceedings of the 2004 ACM SIGGRAPH/Eurographics symposium on Computer animation. Eurographics Association, 2004, pp. 29–37.
25. Sueda, S.; Kaufman, A.; Pai, D.K. Musculotendon simulation for hand animation. *ACM Transactions on Graphics (TOG)*. ACM, 2008, Vol. 27, p. 83.
26. Sigal, L.; Balan, A.O.; Black, M.J. Humaneva: Synchronized video and motion capture dataset and baseline algorithm for evaluation of articulated human motion. *International journal of computer vision* **2010**, *87*, 4.
27. Knight, H.; Simmons, R. Expressive motion with  $x$ ,  $y$  and  $\theta$ : Laban effort features for mobile robots. The 23rd IEEE International Symposium on Robot and Human Interactive Communication. IEEE, 2014, pp. 267–273.
28. Etemad, S.A.; Arya, A. Expert-Driven Perceptual Features for Modeling Style and Affect in Human Motion. *IEEE Transactions on Human-Machine Systems* **2016**, *46*, 534–545.
29. Russell, J.A.; Fehr, B. Relativity in the perception of emotion in facial expressions. *Journal of Experimental Psychology: General* **1987**, *116*, 223.
30. Heimerdinger, M.; LaViers, A. Influence of Environmental Context on Recognition Rates of Stylized Walking Sequences. *9th International Conference on Social Robotics (ICSR)* **2017**.
31. Bartenieff, I.; Lewis, D. *Body Movement: Coping with the Environment*; Gordon and Breach Science Publishers, 1980.
32. Studd, K.; Cox, L. *Everybody is a Body*; Dog Ear Publishing, 2013.
33. Felleisen, M. On the expressive power of programming languages. *Science of computer programming* **1991**, *17*, 35–75.
34. Veltman, J.A.; Brunner, H.G. Understanding variable expressivity in microdeletion syndromes. *Nature genetics* **2010**, *42*, 192.
35. Restle, F. Coding theory of the perception of motion configurations. *Psychological Review* **1979**, *86*, 1.
36. LaViers, A.; Cuan, C.; Maguire, C.; Bradley, K.; Brooks Mata, K.; Nilles, A.; Vidrin, I.; Chakraborty, N.; Heimerdinger, M.; Huzaifa, U.; others. Choreographic and somatic approaches for the development of expressive robotic systems. *Arts. Multidisciplinary Digital Publishing Institute*, 2018, Vol. 7, p. 11.
37. Blum, M.; Kozen, D. On the power of the compass (or, why mazes are easier to search than graphs). *Foundations of Computer Science, 1978., 19th Annual Symposium on*. IEEE, 1978, pp. 132–142.
38. Donald, B.R. On information invariants in robotics. *Artificial Intelligence* **1995**, *72*, 217–304.
39. Elgin, C. Exemplification et la Danse. *Philosophie de la Danse. Rennes: Presses Universitaires de Rennes* **2010**, pp. 81–98.
40. Turing, A.M. On computable numbers, with an application to the Entscheidungsproblem. *J. of Math* **1936**, *58*, 5.
41. Schaller, R.R. Moore’s law: past, present and future. *IEEE spectrum* **1997**, *34*, 52–59.
42. McMahon, T.A.; Bonner, J.T. *On size and life*; Scientific American Library, 1983.
43. Changizi, M.A. Relationship between number of muscles, behavioral repertoire size, and encephalization in mammals. *Journal of Theoretical Biology* **2003**, *220*, 157–168.
44. Immerman, N. Computability and Complexity. In *The Stanford Encyclopedia of Philosophy*, Spring 2016 ed.; Zalta, E.N., Ed.; Metaphysics Research Lab, Stanford University, 2016.
45. Petzold, C. *The annotated Turing: a guided tour through Alan Turing’s historic paper on computability and the Turing machine*; Wiley Publishing, 2008.
46. Choset, H.; Hutchinson, S.; Lynch, K.; Kantor, G.; Burgard, W.; Kavraki, L.; Thrun, S. *Principles of robot motion: theory, algorithms, and implementation*; The MIT Press, 2005.

47. Stephens, G.; Johnson-Kerner, B.; Bialek, W.; Ryu, W. Dimensionality and dynamics in the behavior of *C. elegans*. *PLoS Comput Biol* **2008**, *4*, e1000028.
48. Stephens, G.; Johnson-Kerner, B.; Bialek, W.; Ryu, W.; Warrant, E. From Modes to Movement in the Behavior of *Caenorhabditis elegans*. *PloS one* **2010**, *5*, 462–465.
49. Stephens, G.; Ryu, W.; Bialek, W. The emergence of stereotyped behaviors in *C. elegans*. *Bulletin of the American Physical Society* **2010**, *55*.
50. Gomez-Marin, A.; Stephens, G.J.; Brown, A.E. Hierarchical compression of *Caenorhabditis elegans* locomotion reveals phenotypic differences in the organization of behaviour. *Journal of The Royal Society Interface* **2016**, *13*, 20160466.
51. Dankert, H.; Wang, L.; Hoopfer, E.D.; Anderson, D.J.; Perona, P. Automated monitoring and analysis of social behavior in *Drosophila*. *Nature methods* **2009**, *6*, 297.
52. Chyb, S.; Gompel, N. *Atlas of Drosophila Morphology: Wild-type and classical mutants*; Academic Press, 2013.
53. Ting, L.H.; Macpherson, J.M. A limited set of muscle synergies for force control during a postural task. *Journal of neurophysiology* **2005**, *93*, 609–613.
54. Sebastiani, A.; Fishbeck, D.W. *Mammalian anatomy: the cat*; Morton Publishing Company, 2005.
55. Range of Joint Motion Evaluation Chart. Technical report, Washington State Department of Social and Health Services, <https://www.dshs.wa.gov/sites/default/files/FSA/forms/pdf/13-585a.pdf>, 2014.
56. Azevedo, F.A.; Carvalho, L.R.; Grinberg, L.T.; Farfel, J.M.; Ferretti, R.E.; Leite, R.E.; Lent, R.; Herculano-Houzel, S. Equal numbers of neuronal and nonneuronal cells make the human brain an isometrically scaled-up primate brain. *Journal of Comparative Neurology* **2009**, *513*, 532–541.
57. Gouaillier, D.; Hugel, V.; Blazevic, P.; Kilner, C.; Monceaux, J.; Lafourcade, P.; Marnier, B.; Serre, J.; Maisonnier, B. Mechatronic design of NAO humanoid. IEEE International Conference on Robotics and Automation., 2009, pp. 769–774.
58. Aldebaran, N. Robotics <http://www.aldebaran-robotics.com/eng>.
59. Echelon. Choreographed Control. Technical report.
60. Journal, L.V.R. Fountains of Bellagio continue to amaze visitors. Technical report.



## Appendix. Applied Examples

In this section, the measure introduced in Section 2 will be applied to some instructive examples: a small humanoid robot and Vegas's Bellagio fountains. Passive systems like the motion of a falling leaf versus a falling brick might also be considered.

### Appendix A.1. Aldebaran NAO Humanoid Robot

Figure A1 and Table A1 outline the basic capabilities of the platform where the sensor resolution (an encoder with  $0.1^\circ$  precision) has been used to determine  $R_i$ .

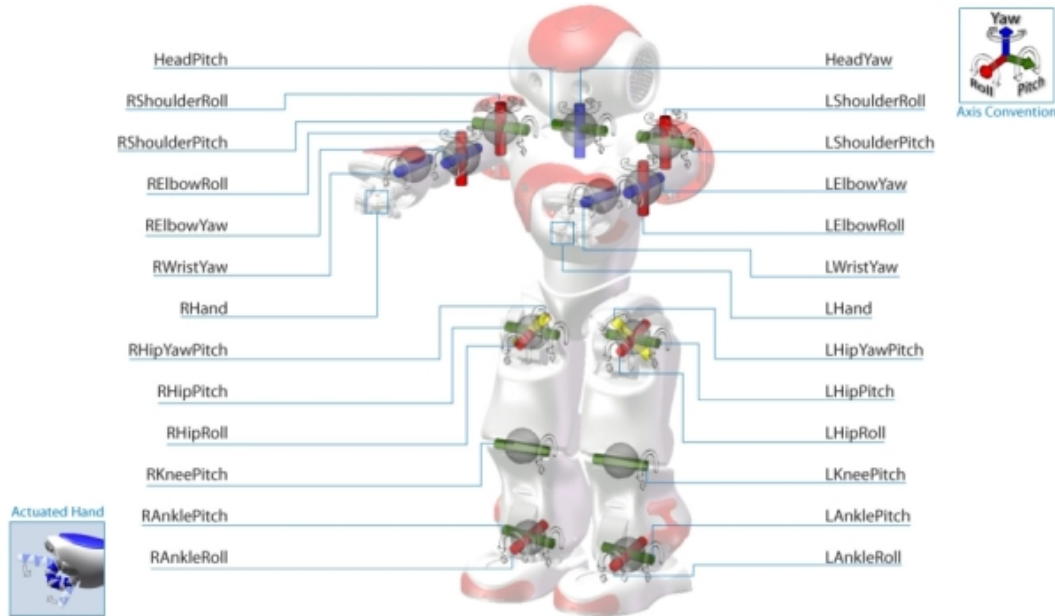


**Figure A1.** A diagram which lists the degrees of freedom on an Aldebaran NAO robot. In addition to these mechanical degrees of freedom the platform contains an ATOM Z530 onboard computer processor, which has 47 million transistors on board. [57,58]

**Table A1.** NAO Aldebaran robot, mechanical degrees of freedom.

DOF	Range / Resolution	$R_i$
l/r hand	open/close	2
head yaw	-119.5 to 119.5 / .1	2390
head pitch (at 0 yaw)	-38.5 to 29.5 / .1	680
l/r shoulder pitch	-119.5 to 119.5 / .1	2390
l/r shoulder yaw	-119.5 to 119.5 / .1	2390
l/r shoulder roll	-88.5 to -2 / .1	865
l/r wrist yaw	-104.5 to 104.5 / .1	2090
pelvis	-65.6 to 42 / .1	1076
l/r hip roll	-21.7 to 45.2 / .1	669
l/r hip pitch	-88 to 27.7 / .1	1157
l/r knee pitch	-5.3 to 121.0 / .1	1263
l/r ankle pitch	-68.2 to 52.9 / .1	1211
l/r ankle roll	-22.8 to 44.1 / .1	669

Thus, the kinematic mechanization capacity is calculated as

$$\mathcal{K} = \log_2(2^2 \times 2390^5 \times 680^1 \times 940^2 \times 865^2 \dots \times 2090^2 \times 1076^1 \times 669^4 \times 1157^2 \times 1263^2 \times 1211^2) \quad (\text{A1})$$

$$= \log_2(4.1 \times 10^{71} \text{ configurations}) \approx 238 \text{ bits}$$

This calculation includes physical combinations which are kinematically or dynamically infeasible. Further, the capacity for changes in motor speed between configurations is not reflected here and would increase the complexity of behavior. Thus, the number may be seen as a static measure.

### Appendix A.2. Bellagio Water Fountains

Consider a tourist attraction, like the Bellagio water fountains in Las Vegas, NV. Tourists line up every hour to watch this famous display, routinely included in lists of popular Vegas attractions. This is to say that the fountain display is visually very interesting, or expressive, for human watchers. The fountain has about 1,200 water cannons with 5,000 lights as part of its display. It also has the ability to create fog and features popular or famous music during the shows. For this analysis [59,60], we'll consider only the water cannons and lights. The cannons come in four types: robotic Oarsman and three sizes of Shooters. The 208 Oarsman are articulated cannons with active control; the Shooters simply blast water at three predetermined pressure settings, each having a single pressure setting according to their size. The lights can be a range of colors.

**Table A2.** Estimated fountain system degrees of freedom.

DOF	Range / Resolution	$R_i$
Oarsmen RX (208)	$0^\circ$ to $160^\circ$ / by $1^\circ$	160
Oarsmen RY (208)	$0^\circ$ to $160^\circ$ / by $1^\circ$	160
Oarsmen water (208)	on/off	2
Shooters (1,175)	on/off	2
lights (6,200)	off or one of 12 colors	13

Table A2 articulates a model for this system. For the Oarsman, which rotate about two axes, we assume a range of motion of  $160^\circ$  with a resolution of  $1^\circ$  in each dimension. We assume the water shooting out of the cannon to be on or off with a single pressure setting. Likewise, the Shooters, are either on or off without articulation. The lights can be 'off' or one of twelve colors (as modeled by a moderate segmentation of the color wheel). We ignore the music that plays alongside.

Thus, to compute the kinematic mechanization capacity, we find the following computation.

$$\mathcal{K} = \log_2(2^{1175+208} \times 160^{208+208} \times 13^{6200}) = \log_2(4.9 \times 10^{8239} \text{ configurations}) \approx 27,372 \text{ bits} \quad (\text{A2})$$

We could argue over which is more interesting to watch: a NAO or the Bellagio fountains, but this metric provides a quantitative bound on *how much more expressive* the fountains are. In this case, about two orders of magnitude with respect to the amount of information they can encode. This result is consistent with expressivity scaling with system expense and tourist attendance.

What if all the water cannons were the articulated, Oarsman variety? In that case, we have:

$$\mathcal{K} = \log_2(2^{1383} \times 160^{1383} \times 13^{6200}) = \log_2(1.2 \times 10^{10371} \text{ configurations}) \approx 34,452 \text{ bits} \quad (\text{A3})$$

Thus, by upgrading 1,175 cannons to the articulated variety, we don't gain much in expressivity. If, in addition, we boost the resolution of each cannon of the original system to  $0.1^\circ$ , we have:

$$\mathcal{K} = \log_2(2^{1383} \times 1600^{1383} \times 13^{6200}) = \log_2(1.2 \times 10^{11754} \text{ configurations}) \approx 39,046 \text{ bits.} \quad (\text{A4})$$

Thus here, we can see how adding water cannons and articulation resolution increases the expressivity of the platform, but we do not capture the additional expressivity that the dynamics of timing and water add to (and take away from) the system. For example, by moving variable speeds, these fountains can create different patterns in the water, which add to the system's expressivity. On the other hand, in the presence of water not all points in the cannon's range might be physically feasible.